ORIGINAL PAPER

Molecular subgrouping of primary pineal parenchymal tumors reveals distinct subtypes correlated with clinical parameters and genetic alterations

Elke Pfaff[1,2,3] · Christian Aichmüller[4] · Martin Sill[1,5] · Damian Stichel[6,7] · Matija Snuderl[8,9,10] · Matthias A. Karajannis[11] · Martin U. Schuhmann[12] · Jens Schittenhelm[13] · Martin Hasselblatt[14] · Christian Thomas[14] · Andrey Korshunov[6,7] · Marina Rhizova[15] · Andrea Wittmann[1,2] · Anna Kaufhold[1,5] · Murat Iskar[4] · Petra Ketteler[16] · Dietmar Lohmann[17] · Brent A. Orr[18] · David W. Ellison[18,19] · Katja von Hoff[20,21] · Martin Mynarek[21] · Stefan Rutkowski[21] · Felix Sahm[1,6,7] · Andreas von Deimling[6,7] · Peter Lichter[4,22] · Marcel Kool[1,5] · Marc Zapatka[4] · Stefan M. Pfister[1,3,5] · David T. W. Jones[1,2]

Abstract

Tumors of the pineal region comprise several different entities with distinct clinical and histopathological features. Whereas some entities predominantly affect adults, pineoblastoma (PB) constitutes a highly aggressive malignancy of childhood with a poor outcome. PBs mainly arise sporadically, but may also occur in the context of cancer predisposition syndromes including *DICER1* and *RB1* germline mutation. With this study, we investigate clinico-pathological subgroups of pineal tumors and further characterize their biological features. We performed genome-wide DNA methylation analysis in 195 tumors of the pineal region and 20 normal pineal gland controls. Copy-number profiles were obtained from DNA methylation data; gene panel sequencing was added for 93 tumors and analysis was further complemented by miRNA sequencing for 22 tumor samples. Unsupervised clustering based on DNA methylation profiling separated known subgroups, like pineocytoma, pineal parenchymal tumor of intermediate differentiation, papillary tumor of the pineal region and PB, and further distinct subtypes within these groups, including three subtypes within the core PB subgroup. The novel molecular subgroup Pin-RB includes cases of trilateral retinoblastoma as well as sporadic pineal tumors with *RB1* alterations, and displays similarities with retinoblastoma. Distinct clinical associations discriminate the second novel molecular subgroup PB-MYC from other PB cases. Alterations within the miRNA processing pathway (affecting *DROSHA*, *DGCR8* or *DICER1*) are found in about two thirds of cases in the three core PB subtypes. Methylation profiling revealed biologically distinct groups of pineal tumors with specific clinical and molecular features. Our findings provide a foundation for further clinical as well as molecular and functional characterization of PB and other pineal tumors, including the role of miRNA processing defects in oncogenesis.

Keywords Pineoblastoma · Molecular subgrouping · Tumors of the pineal region · miRNA processing pathway

✉ David T. W. Jones
david.jones@kitz-heidelberg.de

Extended author information available on the last page of the article

Introduction

Tumors arising in the pineal region are rare, accounting for 0.8–3.2% of primary brain and CNS tumors in children and adolescents [22, 35]. Tumors presumably originating from pineal cells comprise pineocytoma (Pin-Cyt), pineal parenchymal tumors of intermediate differentiation (PPTID), papillary tumors of the pineal region (PTPR) and pineoblastoma (PB) [30]. Further tumor entities occurring in the pineal region include germinomas, gliomas, and metastases.

Pin-Cyt is a low-grade tumor (WHO grade I), accounting for approximately 20% of primary pineal tumors and

typically occurring in adults in their forties. After total surgical resection, prognosis is favorable [30, 39].

Pineal parenchymal tumors of intermediate differentiation have clinical and morphological features intermediate between Pin-Cyt and PB and correspond to WHO grade II-III with definitive grading criteria still pending. Therefore, diagnosis can be challenging [30].

Papillary tumors of the pineal region are very rare neuroepithelial tumors affecting children and adults (mean age at diagnosis 35 years) and often recur locally [30]. By DNA methylation-based clustering, two distinct subtypes within PTPR are distinguished. Although no significant difference with regards to clinical and histopathological features or molecular alterations have been identified to date, there is a trend to a longer survival for one of the subtypes [19]. Typical alterations found in PTPR are loss of chromosomes 3, 10 and 22q, gain of chromosomes 8 and 12 as well as *PTEN* alterations [16].

PB mainly occurs in children and young adults and accounts for approximately 5% of childhood brain tumors. It is an embryonal tumor graded as WHO grade IV which frequently disseminates in the cranio-spinal axis [15, 30]. Formerly, PB were frequently termed pineal 'primitive neuroectodermal tumor of the central nervous system' (CNS-PNET) [27]—however, more recent studies could show that 'PNET' in the pineal gland and elsewhere in the CNS are classified into distinct molecular entities [31, 44].

Despite multimodal treatment regimens with postsurgical polychemotherapy and cranio-spinal irradiation [13, 32], the median overall survival is relatively short (with 10-year overall survival rates of 48.6% in a series of 31 cases [10]), especially for children less than 4–5 years of age at diagnosis [32, 36].

Data on the comprehensive molecular characterization of PB and correlation with the clinical course of the patients are rare to date. Previous reports on copy-number analysis in PB included only small sample series [3, 23, 27, 31, 45]. To our knowledge, we present here one of the first studies on DNA methylation analysis in PB as well as one of the largest cohorts of this tumor type studied so far.

PB can be linked to genetic predisposition when arising in a rare condition called 'trilateral retinoblastoma syndrome' (TLRB) with an underlying *RB1* germline mutation and co-occurring uni- or bilateral retinoblastoma [6, 7, 48]. Further, PB is one of the various tumor types that can occur in the context of patients with DICER1 Syndrome harboring a *DICER1* germline mutation [40, 41]. Somatic *DICER1* mutations and homozygous deletions of *DROSHA* have also been described in PB [8, 43], suggesting a possible role for miRNA processing defects in PB tumorigenesis.

MicroRNAs (miRNA) are small, non-coding RNA molecules which exert a regulatory effect on their mRNA targets. The complex formed by the nuclear ribonuclease DROSHA and the microprocessor complex subunit DGCR8 further processes primary precursor miRNA into hairpin precursor-miRNA, which is then cleaved by DICER1 to obtain mature miRNA [42].

Herein, we describe the molecular classification of 195 pineal tumors based on DNA methylation patterns into known subgroups. Moreover, we present the delineation of novel molecular subgroups as well as subtypes associated with distinct clinical characteristics and molecular alterations. Importantly, we find defects in the miRNA processing pathway in at least 40% of PBs.

Material and methods

Sample selection and clinical data

Tumor samples were obtained from international collaboration partners as either fresh frozen or formalin-fixed paraffin-embedded (FFPE) tissue samples. The majority of tumor samples were histologically diagnosed as pineal tumors, however, no central histopathological review was performed due to the diverse origins of this retrospective series.

Two PB samples were first and second relapse, respectively. For all other samples no explicit information was available, but it is assumed that these samples are primary disease and therefore treatment-naïve. Normal pineal gland samples were partly primarily diagnosed as Pin-Cyt (5/20) or PPTID (1/20) that were later found to have minimal/no tumor content. The remaining samples were collected postmortem from patients who died from other causes (not a pineal tumor).

Clinical data and tumor material were obtained according to local ethical and institutional review board approval and collected at the German Cancer Research Center (DKFZ, Heidelberg, Germany). Informed consent for molecular profiling was obtained from all patients and/or their legal representatives. A proportion of cases was previously published in Capper et al. [4] or Hwang et al. [21], but the majority of cases were collected within the scope of collaborative research efforts, international molecular diagnostic studies or routine histopathological and molecular diagnostic assessment.

DNA methylation profiling

Genome-wide DNA methylation profiles were obtained using Illumina Infinium HumanMethylation450 (450 k) array and Illumina Infinium MethylationEPIC (EPIC) array, according to the manufacturer's instructions (Illumina, San Diego, USA). Data were generated at the Genomics and Proteomics Core Facility of the DKFZ (Heidelberg, Germany) and St. Jude Children's Research

Hospital (Memphis, USA). On-chip quality metrics of all samples were carefully controlled. The conumee Bioconductor package version 1.12.0 was used for copy-number variation (CNV) analysis from 450 k and EPIC methylation array data. All computational analyses were performed in R version 3.4.4 (R Development Core Team, 2019). The minfi Bioconductor package version 1.24.0 was applied for determination of raw signal intensities obtained from IDAT-files. Selecting the intersection of probes present on both arrays (combineArrays function, minfi) was used for merging Illumina EPIC and 450 k samples to a combined data set. Individual normalization was performed for each sample using a background correction (shifting of the 5th percentile of negative control probe intensities to 0) and a dye-bias correction (scaling of the mean of normalization control probe intensities to 10,000) for both color channels. Subsequently, a correction for the type of material tissue (FFPE/frozen) and array (450 k/EPIC) was applied by fitting univariate, linear models to the log2-transformed intensity values (removeBatchEffect function, limma package version 3.34.5). Correction was performed individually for methylated and unmethylated signals. Beta-values were calculated from the retransformed intensities using an offset of 100 (as recommended by Illumina). The following filtering criteria were applied before further analyses were performed: Removal of probes targeting the X and Y chromosomes ($n = 11{,}551$), removal of probes containing a single-nucleotide polymorphism (dbSNP132 Common) within five base pairs of and including the targeted CpG-site ($n = 7998$), probes not mapping uniquely to the human reference genome (hg19) allowing for one mismatch ($n = 3965$), and 450 k array probes not included on the EPIC array. In total, 428,230 probes were kept for downstream analysis. To perform unsupervised dimension reduction, the remaining probes were used to calculate the 1-variance weighted Pearson correlation between the samples. For t-SNE analysis (t-Distributed Stochastic Neighbor Embedding; Rtsne package version 0.13) the resulting distance matrix was used as input. The following non-default parameters were applied: theta = 0, pca = F, max_iter = 2500 perplexity = 20. For unsupervised hierarchical clustering, the 10.000 probes with highest standard deviation were selected to calculate the Euclidean distance between samples, followed by applying Wards linkage method for sample clustering. In the heatmap, reordering of representation probes by complete linkage hierarchical clustering of the Euclidean distance between probes was conducted. Copy-number profiles of each case were visually inspected for evaluation of focal amplifications and deletions and chromosomal gains and losses. Candidate genes and their 3′ and 5′ intergenic neighborhood were further investigated using the Integrative Genomic Viewer (IGV) for the presence of breakpoints, as an indication for potential gene fusions.

Next-generation sequencing

An updated version of a previously described customized enrichment/ hybrid-capture-based next-generation sequencing (NGS) gene panel including a selection of genes recurrently altered in brain tumors was applied [38] in a total of 93 samples (28×PB-Group 1A (PB-Grp1A), 4×PB-Group 1B (PB-Grp1B), 7×PB-Group 2 (PB-Grp2), 6×PB-MYC (pineoblastoma with *MYC* alterations), 8×Pin-RB (pineal tumors with *RB1* alterations), 9×Pin-Cyt, 9×PPTID-A, 7×PPTID-B, 3×PTPR-A, 12×PTPR-B). Furthermore, low-coverage whole-genome and whole-exome sequencing according to the INFORM pipeline were performed for two samples as described elsewhere [47]. The following filtering settings were applied for gene panel sequencing data, since no germline material was available for analysis: only exonic, nonsynonymous single-nucleotide variants (SNV) with a frequency of ≤ 0.01 in the 1000 genomes database (https://www.internationalgenome.org/) were considered. Furthermore, SNVs were excluded when (1) the respective SNV was listed in the dbSNP database (https://www.ncbi.nlm.nih.gov/projects/SNP/) but not in the COSMIC database (https://cancer.sanger.ac.uk/cosmic), (2) when ≥ 10% of SNV counts in one gene were exactly the same specific nucleotide substitution found within different subtypes, and (3) when the specific SNV was listed as a benign variant in the ClinVar database (https://www.ncbi.nlm.nih.gov/clinvar/).

miRNA sequencing and clustering

The small RNA composition of a total of 22 samples (9×PB-Grp1A, 1×PB-Grp1B, 1×PB-Grp2, 3×PB-MYC, 5×PPTID-A, 3×PPTID-B) was obtained by sequencing on an Illumina HiSeq2000 applying Illumina's NEBNext Small RNA protocol using 50 bp single-end reads. For miRNA clustering gene counts based on uniquely mapped reads have been normalized using the 'rlog' function from the R-package (https://genomebiology.biomedcentral.com/articles/10.1186/s13059-014-0550-8). Based on standard deviation, the most variable 15% miRNA have been chosen for clustering. To measure individual miRNA expression as deviation from the cohort mean expression, a z-transformation has been applied. For clustering, spearman correlation has been used to measure similarity and agglomeration was done according to ward.D.

smallRNA alignment

Reads were aligned to a masked version of the human genome version 19 (hg19/ GRCh37). Only regions harboring

smallRNA and long non-coding RNA were accessible for alignment. Genetic locations were annotated using GEN-CODE gene annotation (version 28, liftover37) [12]. miRNA annotations were replaced with annotations provided by MiRBase (version 20) [25].

Sequencing reads were aligned using STAR version 2.5.2 with a parameter setting suggested by ENCODE [5]. Additionally, reads were aligned to a miRNA genome provided by MiRBase using BOWTIE2, version 2.3.4.3, using the parameter configuration -phred33, -D 20, -R 3, -N 0, -L 8, -i S, 1, 0.50.

Statistical analysis

Statistical analysis was conducted using R, version 3.4.4.

Results

Separation of distinct groups of pineal tumors based on DNA methylation patterns

Samples for the current cohort were selected based on DNA methylation profiling applying a previously proposed classification algorithm [4] and including samples with the highest score for one of the pineal subgroups. 149/195 (76.4%) pineal tumor samples reached a DNA methylation score of at least 0.9 for one of the pineal subgroups according to the classification algorithm, whereas the score for one of the pineal subgroups was 0.22–0.89 for 28/195 (14.3%) cases. 13 samples were assigned to the methylation class "medulloblastoma, subclass group 3" with scores of 0.25–0.99. These tumors were primarily diagnosed as PB or PNET and therefore included in this study. Two cases with the highest score for the methylation class "retinoblastoma" (score 0.61 and 0.99, respectively) were primarily diagnosed as PNET and PB and fall into the subgroups PB-MYC and Pin-RB in this study, respectively. A small number of additional samples with low classifier scores were included in further clustering analyses on an exploratory basis due to their initial diagnosis as pineal tumors.

Unsupervised clustering based on DNA methylation patterns of 195 tumor samples as well as 20 normal tissue samples from the pineal region (Norm-Pin, median age of 44 years, range 12–81, not age-matched) revealed distinct entities—Pin-Cyt, PPTID, PTPR and PB (Fig. 1). Distinct subtypes within the respective subgroups [like PB-Grp1A, PB-Grp1B and PB-Grp2 within the PB subgroup as well as two different subtypes within the PPTID and PTPR groups (subtypes A and B, respectively)] as well as two novel molecular subgroups within the PB group [named Pin-RB (pineal tumors with *RB1* alteration) and PB-MYC (PB with *MYC* activation)] could be distinguished since they formed

distinct clusters based on t-distributed stochastic neighbor embedding (Fig. 1a). Separation of the defined subtypes could be reproduced by hierarchical clustering using 10,000 probes filtered based on standard deviation (Fig. 1b). Gross subgroup affiliation was stable applying variable probe numbers. Information on demographics and clinical follow-up for all subgroups and subtypes are given in Table 1 and illustrated in Fig. 2.

Pineal parenchymal tumors of intermediate differentiation ($n = 27$) as a distinct molecular subgroup can be separated into two further subtypes based on methylation profiling. Tumors of both subtypes showed relatively flat copy-number profiles with broad gains or losses in some cases (illustrated in Fig. 3). Recent reports describe *KBTBD4* small in-frame insertions as recurrent and characteristic alterations in PPTID as well as Group 3 and Group 4 medulloblastoma (MB-G3, MB-G4) [26, 33]. In line with these findings, we identified small insertions in *KBTBD4*, the Kelch repeat- and BTB domain-containing protein 4, in all PPTID cases with gene panel sequencing data available (9 × PPTID-A and 7 × PPTID-B). 11 cases harbored the specified in-frame insertion p.R313delinsPRR described in MB and PPTID [26, 33] whereas five cases showed an insertion of 9 instead of 6 bases in the same genomic region at codons 313–314 within a Kelch repeat domain.

For the PTPR group ($n = 46$) we could discriminate two separate subtypes (Fig. 1a, b), as previously described by Heim et al. [19]. The most frequently occurring alteration was loss of chromosome 10 in 83% of cases (10/12) of the PTPR-A subtype and 97% of cases (33/34) of the PTPR-B subtype (Fig. 3a). In the PTPR-B subtype, two cases (2/12 with gene panel sequencing data available) harbored a small insertion/deletion (InDel) resulting in a frameshift in PTEN and one further PTPR-B case showed a homozygous deletion of the *PTEN* gene locus. No *PTEN* alterations were observed in tumors of the PTPR-A subtype. Chromosome 10 loss and *PTEN* alterations were previously described in PTPR [19].

Samples of the Pin-RB molecular entity cluster close to retinoblastoma and frequently harbor *RB1* alterations

A distinct molecular subgroup designated Pin-RB ($n = 16$) emerged from the clustering (Fig. 1). Tumor samples known to have arisen in the context of 'trilateral retinoblastoma' (TLRB) fell into this subgroup, but did not form a distinct subcluster separate from the other Pin-RB samples without this specific information (Fig. 1c).

Patients of the Pin-RB subgroup were on average significantly younger compared to the core PB subtypes PB-Grp1A, PB-Grp1B and PB-Grp2 (Fig. 2a). Gender distribution and primary diagnosis are illustrated in Fig. 2b + c.
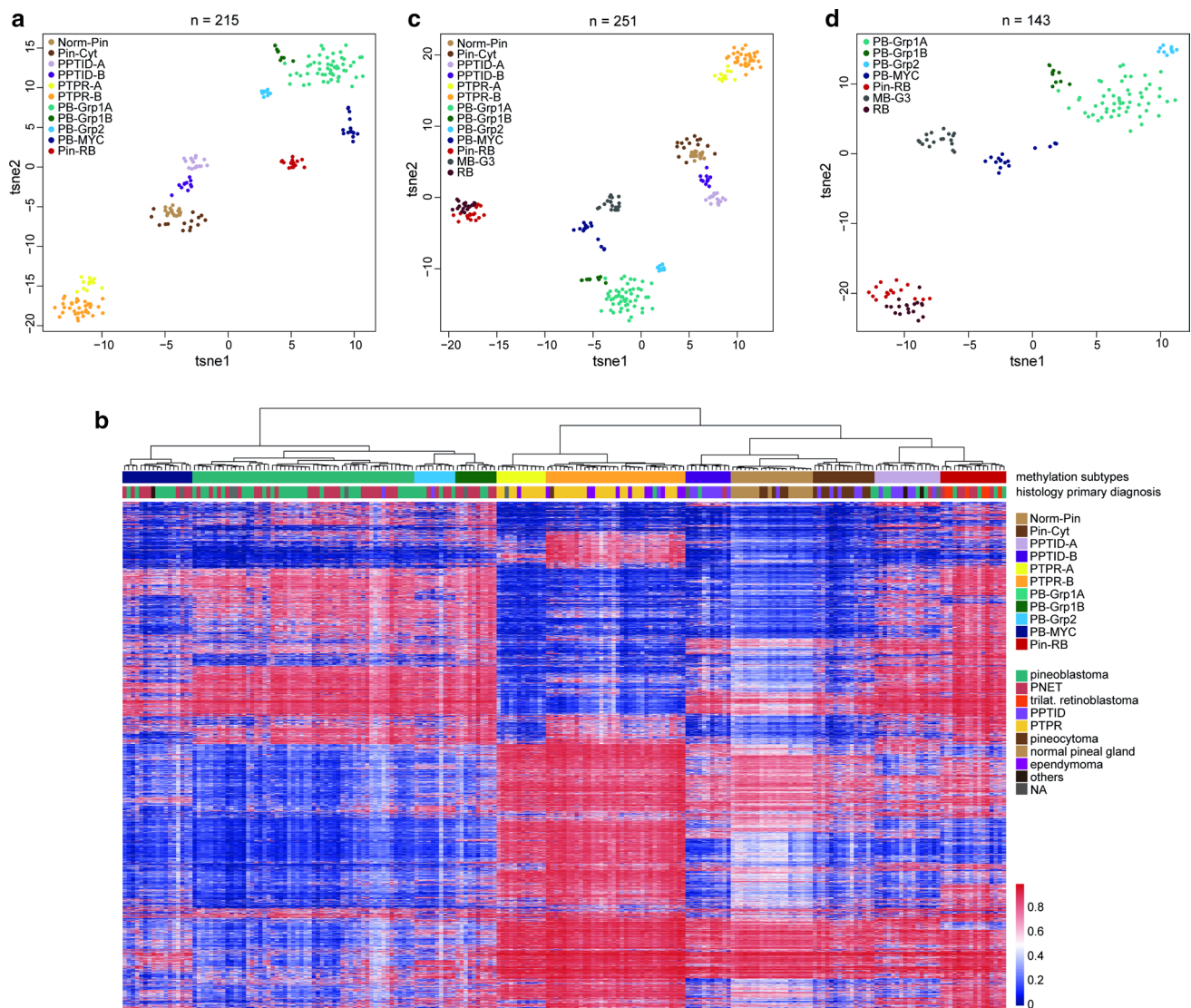
Fig. 1 Separation of distinct subgroups and further subtypes of pineal tumors by t-distributed stochastic neighbor embedding plot (**a**) and hierarchical clustering (**b**). Pin-RB form a cluster with retinoblastoma and PB-MYC cluster next to MB-G3 (**c**, **d**). *Norm-Pin* normal pineal gland tissue, *Pin-Cyt* pineocytoma, *PPTID* pineal parenchymal tumor of intermediate differentiation, *PTPR* papillary tumor of the pineal region, *PB* pineoblastoma, *TLRB* trilateral retinoblastoma, *MB-G3* medulloblastoma group 3, *RB* retinoblastoma

RB1 alterations (SNVs, InDels) were found in 9/10 cases with sequencing data available or known mutation status, with the *RB1* mutation being confirmed as somatic in at least one case (no germline data available for the remaining cases). Variant allele frequencies ranged from 47–100%. Two cases harbored a homozygous focal *RB1* deletion. Altogether, 11/16 cases showed an *RB1* alteration (SNV, InDel or gene deletion) predicted to lead to a loss of function (with sequencing data missing for 6 cases).

Information on *RB1* germline status was known for three of the TLRB cases, with a constitutional heterozygous *RB1* germline alteration accompanied by loss-of-heterozygosity (LOH) in the tumor in each case. One further

TLRB case harbored an *RB1* stopgain mutation without germline data available.

As another highly recurrent alteration, loss of chromosome 16q was identified in 11/16 (69%) cases in the Pin-RB group with concomitant chromosome 16p loss being less frequently observed (8/16, 50%). Furthermore, 9/16 (56%) cases displayed a gain of chromosome arm 1q (Fig. 3a, b). Besides *RB1* alterations, these chromosomal changes are recurrent findings in retinoblastoma—with chromosome 1q gain described in 57% and loss of chromosome 16 found in 11–23% [17, 18, 28].

The similarity of Pin-RB and retinoblastoma regarding DNA methylation patterns was further illustrated when a

Table 1 Demographical and clinical information

Characteristics	PB-Grp1A	PB-Grp1B	PB-Grp2	PB-MYC	Pin-RB	PPTID-A	PPTID-B	PTPR-A	PTPR-B	Pin-Cyt
Total number	54	10	10	17	16	16	11	12	34	15
Gender										
Female	40	3	3	5	7	7	9	8	15	10
Male	14	7	7	12	9	9	2	4	19	5
Age—median (range)	11 (3–23)	12 (6–15)	11 (9–17)	1 (0.3–7)	2 (0.1–3.8)	42 (11–64)	58 (17–61)	36 (10–63)	18.5 (0.5–46)	55.5 (27–70)
NA	19	5	4	8	3	3	4	3	8	5
Primary diagnosis (%)										
PB	26	2	5	7	4	5	1	0	1	1
PNET	24	7	4	8	6	1	1	0	0	0
PPTID	1	0	1	0	0	7	8	0	1	5
PTPR	0	0	0	0	0	0	0	10	21	0
Pin-Cyt	0	0	0	0	0	0	0	0	0	9
TLRB	0	0	0	0	6	0	0	0	0	0
EPN	0	0	0	0	0	0	0	1	10	0
Others	0	0	0	1	0	1	0	0	1	0
NA	3	1	0	1	0	2	1	1	0	0
Follow-up										
Progression yes	4	1	0	5	3	1	1	2	8	NA
PFS (mean months)	58.1	18	16	12.3	60.5	41	7.5	76.2	47.4	NA
Death yes	4	1	0	4	4	1	0	1	3	NA
OS (mean months)	59.2	35	16	14.8	52.8	42.5	73.5	88.5	72.3	NA
NA	41 (1 no PFS)	9	7	10 (1 no OS)	8 (2 no PFS)	14	9	6	20	15

NA not available, *PB* pineoblastoma, *PNET* primitive neuroectodermal tumor, *PPTID* pineal parenchymal tumor of intermediate differentiation, *PTPR* papillary tumor of the pineal region, *Pin-Cyt* pineocytoma, *TLRB* trilateral retinoblastoma, *EPN* ependymoma, *PFS* progression-free survival, *OS* overall survival
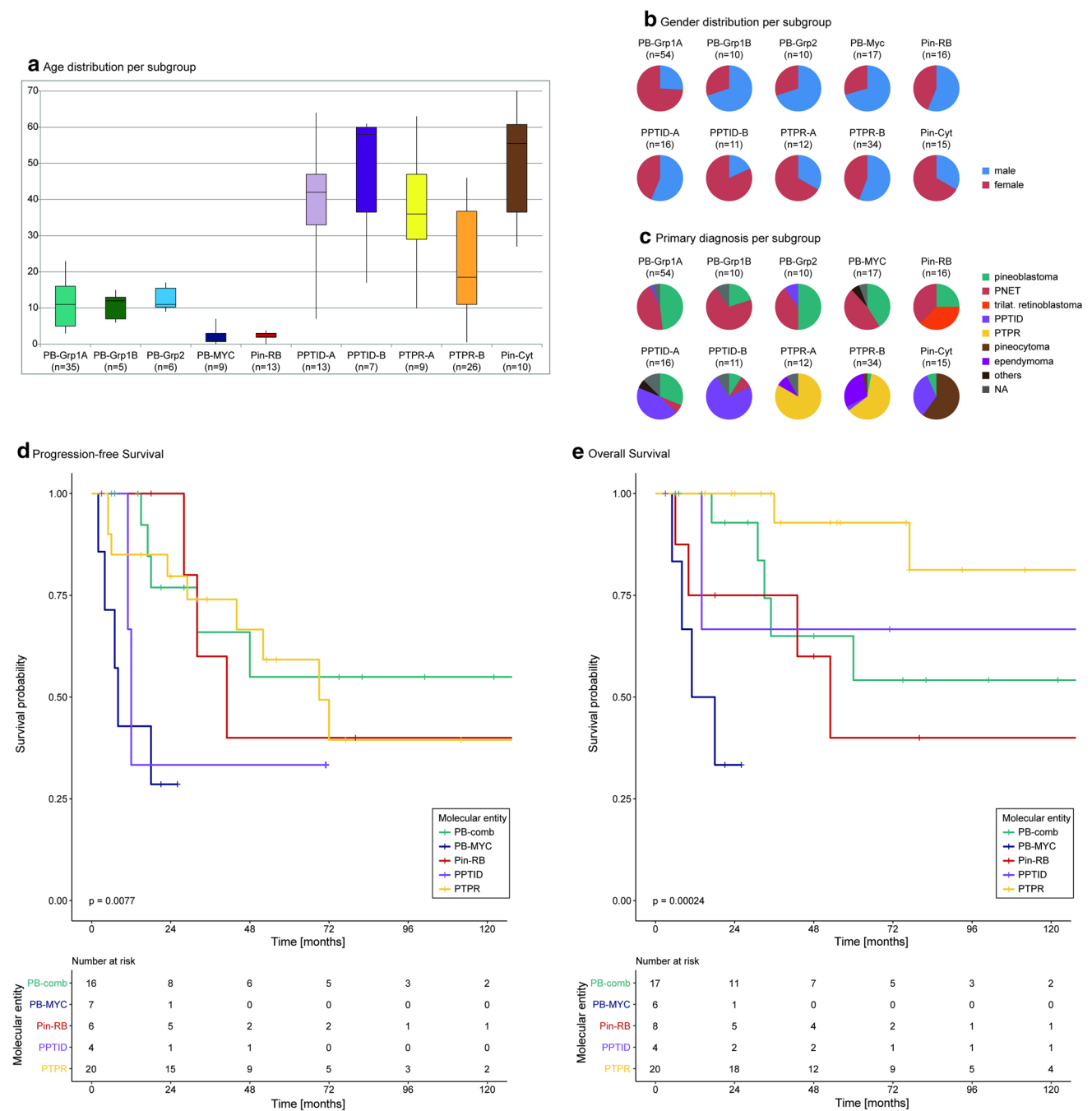
Fig. 2 Patients of the PB subtypes are older compared to PB-MYC and Pin-RB. PPTIDs and PTPR are mainly diagnosed in adult patients (**a**; numbers indicate cases with information on age available). Gender distribution (partly based on gender prediction from genome-wide methylation analysis) (**b**) as well as histological primary diagnosis (**c**) are illustrated per subgroup and subtype. Kaplan–Meier curves for progression-free (**d**) and overall (**e**) survival suggest differences in outcome between the subtypes/subgroups. *PB-comb* PB-Grp1A, PB-Grp1B and PB-Grp2 combined

cohort of 18 retinoblastoma cases was included in the clustering for comparison. Pin-RB samples and typical ocular retinoblastoma fall into the same cluster (Fig. 1c + d), likely indicating commonalities in their cellular origin and pointing to the intriguing evolutionary resemblance of the pineal gland and the retina.

A new molecular subgroup named PB-MYC shows similarities with Group 3 medulloblastoma

As for the Pin-RB cases, patients of the second newly emerging molecular subgroup named PB-MYC—due to evidence of MYC activation—were on average significantly younger
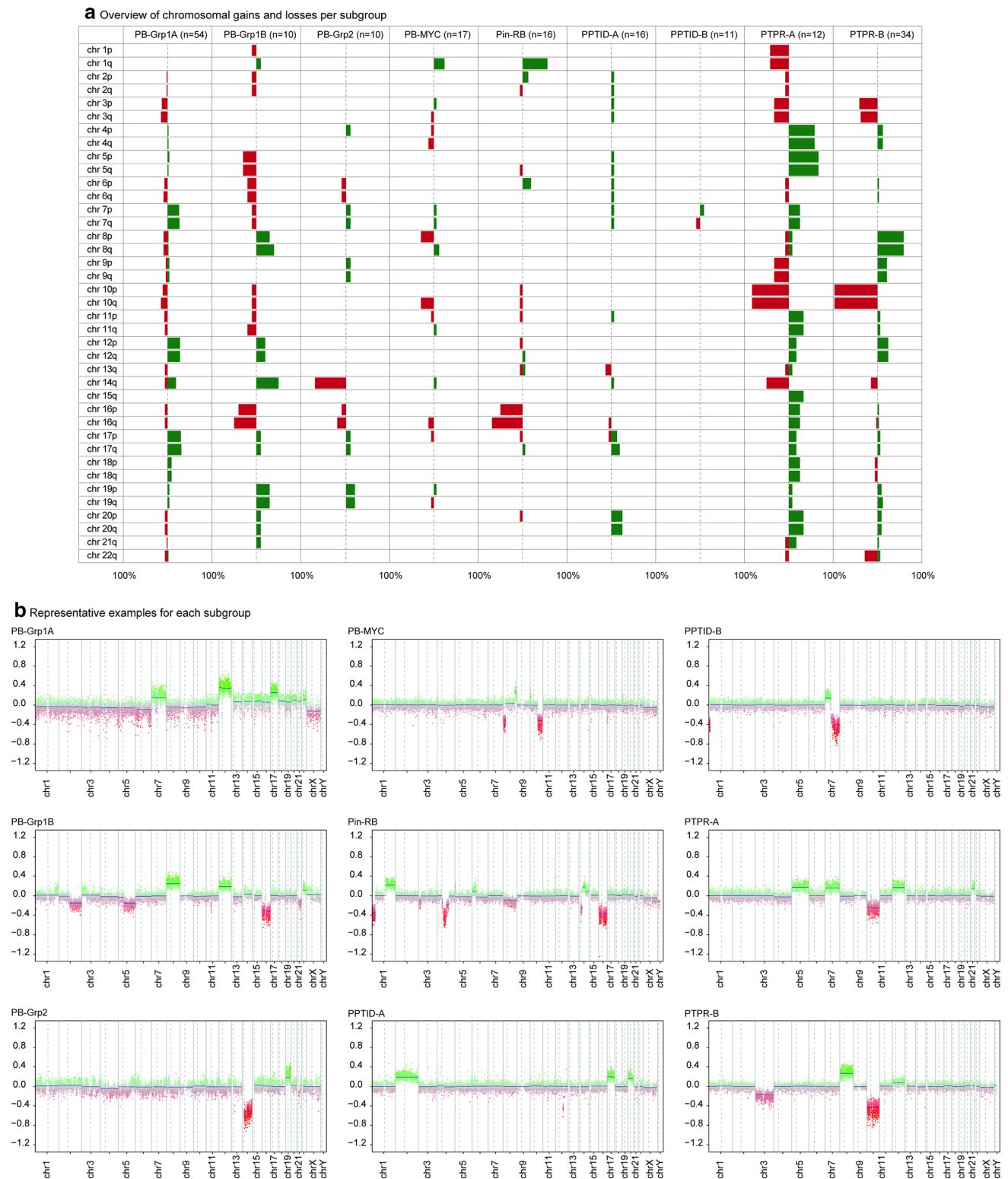
Fig. 3 Overview of chromosomal aberrations with gains and losses of chromosomal arms shown as percentages of cases per subtype harboring the respective alteration (**a**) and representative examples for each subtype (**b**)

at diagnosis compared to the three core PB subtypes PB-Grp1A, PB-Grp1B and PB-Grp2 (Fig. 2a). Recurrent copy-number alterations included complete loss of chromosome 8p and loss of chromosome 10q, each in 5/17 cases (29%) (Fig. 3). Notably, *MYC* amplification was identified in two cases and a broader chromosomal gain including the *MYC* gene locus in three further cases, summing up to *MYC* alterations being found in 5/17 PB-MYC cases (29%). MB-G3, another primitive embryonal tumor, is also known to be MYC-driven [34]. Based on DNA methylation patterns, the cluster of PB-MYC tumors delineates close to but still separated from the MB-G3 cluster (*n* = 18) (Fig. 1c + d). In contrast to the three other PB subtypes (see below), no alterations in the miRNA processing pathway were identified in PB-MYC tumors, with gene panel data being available for 6/17 cases. Furthermore, no alterations in *KBTBD4* were observed in any of the PB-MYC cases, as might have been suspected by the findings of Northcott et al. [33] with *KBTBD4* alterations as characteristic for MB-G3 and MB-G4. Based on the data presented here, the molecular subgroup PB-MYC appears to be clearly distinct from the other pineal tumor groups. Due to small sample numbers, however, an independent replication will be necessary in future.

Discrimination of three distinct subtypes of pineoblastoma with specific clinical features and genetic alterations

When focusing further on the remaining PB cluster, three different subtypes can be distinguished (named PB-Grp1A, PB-Grp1B, PB-Grp2) (Fig. 1a + b) with PB-Grp1A and -1B falling close together. Patients' age, gender distribution and primary diagnosis are illustrated in Fig. 2a, c.

Within PB-Grp1A (*n* = 54) recurrent homozygous focal deletion of the *DROSHA* or *DGCR8* gene loci were identified in 11/54 (20%) and 4/54 (7%) cases, respectively (example depicted in Fig. 4a + b), whereas none of the PB-Grp1B (*n* = 10) tumors showed a deletion of one of these genes.

Sequencing analysis (available for 29 PB-Grp1A and 4 PB-Grp1B cases) revealed *DROSHA* mutations in 3/29 (10%) PB-Grp1A cases. *DICER1* mutations were detected in 6/29 (21%) PB-Grp1A cases and 3/4 (75%) PB-Grp1B cases (three cases harbored two *DICER1* alterations) (Fig. 4d). Eight of the detected *DICER1* mutations were not previously listed in common databases. Four *DICER1* alterations were described before as being pathogenic in a germline context (https://www.ncbi.nlm.nih.gov/clinvar; SCV000267168.1; SCV000581544.3; SCV000581563.3; accession date 03/25/2019). Four of the detected *DICER1* mutations are located within the Ribonuclease IIIA domain (Fig. 4e) [20]. All other *DICER1* alterations are outside functional domains—as previously described in PB, but in contrast to other tumor entities where somatic *DICER1* mutations typically cluster within the Ribonuclease IIIB domain [8, 11]. Variant allele frequencies for *DICER1* as well as *DROSHA* mutations varied from 30–99%. Two cases in our series were known to harbor a *DICER1* germline mutation. For all other cases, discrimination between somatic or germline mutation status could not be made due to lack of available germline material. One case harboring a *DICER1* stopgain mutation showed a further pathogenic *NRAS* hotspot mutation as well as focal high-level *CDK6* and *MYC* amplification.

PB-Grp1B tumors harbored several whole-chromosome gains and losses (Fig. 3), with chromosome 8 gain and chromosome 16 loss as the more frequent ones. Gain of chromosome 14q (being observed in 50% of cases, 5/10) was more specific but not exclusive for this subtype.

For the third specific subtype of PB, PB-Grp2 (*n* = 10), loss of chromosome 14q was the most frequent alteration, being found in 7/10 cases (70%) (Fig. 3). Furthermore, two cases of this subtype showed homozygous focal deletion of the *DROSHA* gene locus. Sequencing analysis revealed frameshift InDels in the *DICER1* gene in two further cases, summing up to alterations in the miRNA processing pathway in 4/7 cases with both sequencing and copy-number data available (Fig. 4).

Taken together, alterations in genes of the miRNA processing pathway (namely *DROSHA*, *DGCR8* and *DICER1* as illustrated in Fig. 4c) were found in 31/74 (41.9%) cases in the core PB subtypes combined (PB-Grp1A, PB-Grp1B, PB-Grp2), with all alterations being mutually exclusive (Fig. 4d). For cases with both copy-number plots and sequencing data available, 23/40 cases (57.5%) harbored an alteration in the miRNA processing pathway.

Results of the next-generation sequencing (NGS) gene panel revealed described alterations in the *DICER1, DROSHA, DGCR8* as well as *RB1* genes. Furthermore, a *NRAS* hot spot mutation and a pathogenic *ATM* mutation were detected each in one PB-Grp1A case. No further recurrent alterations which were considered to play a relevant role in the pathogenesis of these tumors were identified. A list of genes included in the gene panel is given as Supplement Table 1 (online resource).

Defects in miRNA processing in PB subtypes lead to global changes in small RNA composition

Due to the observed alterations in the miRNA processing pathway in PBs, we performed miRNA sequencing in a cohort of 22 pineal samples (9 × PB-Grp1A, 1 × PB-Grp1B, 1 × PB-Grp2, 3 × PB-MYC, 5 × PPTID-A, 3 × PPTID-B) as well as 3 normal brain and 6 MB-G4 samples as controls (Fig. 4f + g).

Unsupervised clustering based on the top 15% most variable miRNAs by standard deviation revealed separate
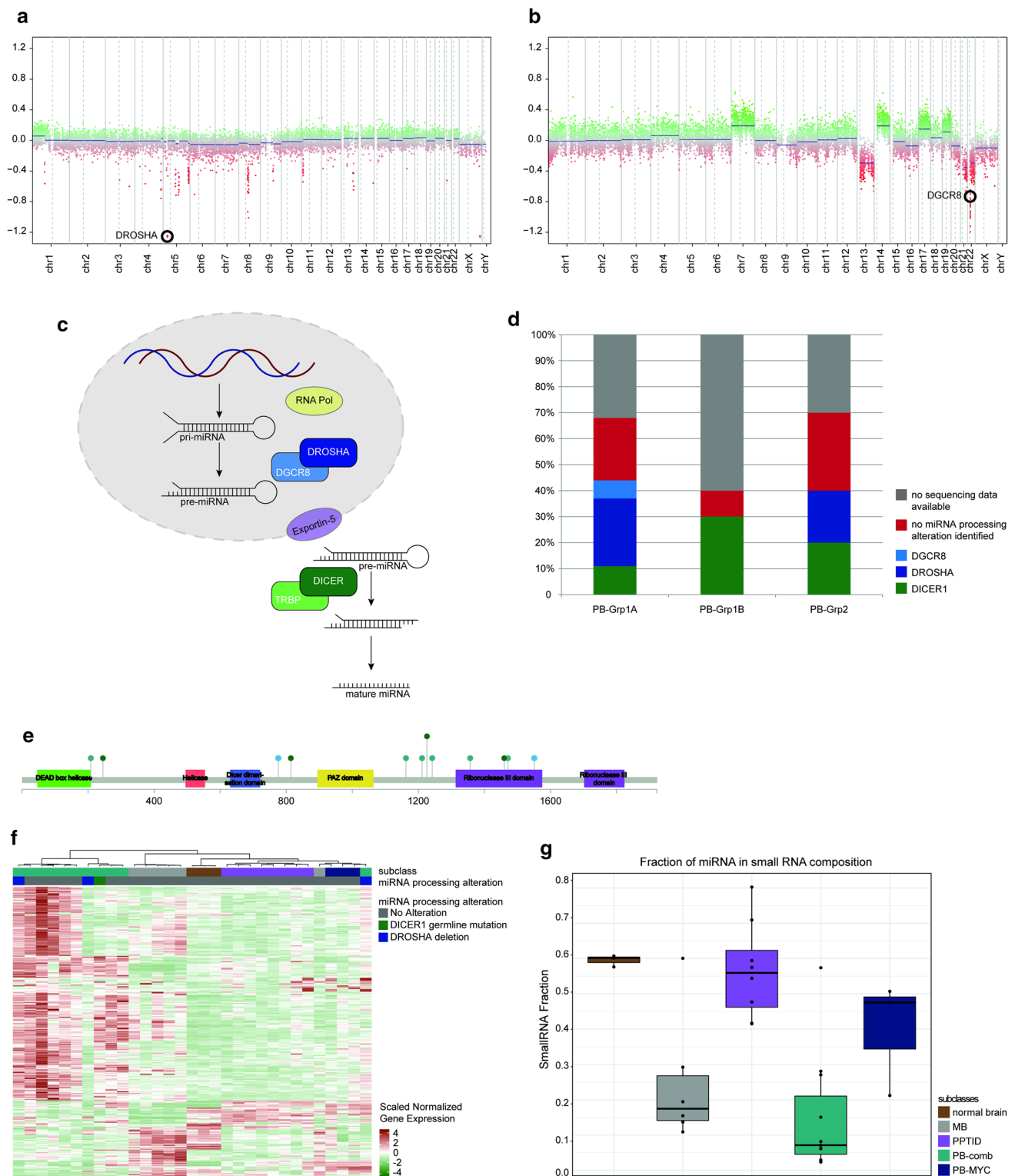
Fig. 4 Focal deletions of *DROSHA* (**a**) and *DGCR8* (**b**) are recurrent findings in the PB subtypes (PB-Grp1A, PB-Grp2). *DROSHA*, *DGCR8* and *DICER1* are key players in the miRNA processing pathway (**c**). Percentages of *DICER1*-, *DROSHA*- and *DGCR8*- altered cases are illustrated for the core PB subtypes (PB-Grp1A, PB-Grp1B, PB-Grp2) (**d**). Localization of detected *DICER1* mutations in corre-

lation to the functional domains (**e**). Unsupervised clustering based on the top 15% most variable miRNAs (distance: Spearman, Agglomeration: ward.D) revealed distinct subtypes (**f**). PB tumors displayed a smaller miRNA fraction compared to PB-MYC, PPTID and normal brain (**g**)

clusters for PB subtypes (PB-Grp1A, PB-Grp1B, PB-Grp2 taken together as PB-combined), PB-MYC samples and PPTID (Fig. 4f). Since subtypes PB-Grp1A, PB-Grp1B and PB-Grp2 form one branch directly from the root of the dendogram based on the hierarchical clustering (Fig. 1b), it seems plausible to combine these subtypes for miRNA analyses. Furthermore, sample numbers were too small to segregate PB-Grp1A, PB-Grp1B and PB-Grp2 subtypes. The proportion of uniquely mapped reads aligning to specific miRNA regions in the genome was significantly lower for the PB subtypes compared to PPTID (but not compared to MB), indicating on average less processed miRNA in the PB subtypes (Wilcoxon Test, FDR < 0.01). PB subtypes showed a lower fraction of miRNA (based on reads aligned to miRNA regions) within the small RNA composition compared to normal brain and PB-MYC, although no statistical test was conducted due to insufficient sample size of the respective subtypes (Fig. 4g). Differences within and between subtypes might be due to quantitative changes of small RNA classes other than miRNA. Further functional investigation will be required to fully elucidate the exact cause for miRNA changes in these tumors.

Comparison of 3′/5′ miRNA expression across samples, irrespective of the subtype, showed an on average slightly higher expression of 5′ miRNA (Supplementary Fig. 1a, online resource). Two PB cases—one carrying a *DICER1* germline mutation—displayed a significant difference in their 3′/5′ miRNA expression ratio (paired Wilcoxon Test, $p < 0.01$) with lower expression of 3′ miRNA.

The fraction of completely processed miRNA in relation to all miRNA was significantly lower for the PB subtypes in comparison to MBs, but not in comparison to PPTIDs (Wilcoxon Test, $fdr < = 0.01$) (Supplementary Fig. 1b, online resource). Supplementary Fig. 1c (online resource) shows the detailed small RNA composition. Due to small numbers of samples with suitable material for analysis, not covering all described alterations in the miRNA processing pathway, a genotype–phenotype correlation was not possible.

Follow-up data suggest unfavorable outcome for the PB-MYC molecular subgroup

Clinical follow-up data were available for 59 tumor patients (see Table 1). Based on Kaplan–Meier analysis, differences in progression-free survival (PFS) as well as overall survival (OS) can be observed (Fig. 2d + e). PPTID and PTPR appear to show a more favorable OS compared with PB, Pin-RB and PB-MYC, despite showing similar relapse rates. Survival curves for both PFS and OS suggest the poorest prognosis in the PB-MYC molecular subgroup. However, patient numbers are currently too small to draw final conclusions or statistically validate the observed trends.

Discussion

Multiple different tumor entities can arise in the pineal gland, with PB (the most aggressive variant) mainly occurring in the pediatric age group. Prognosis for PB is quite poor despite multimodal therapy, and little is known about underlying genetic alterations or molecular subgroups.

With our study presented here, we confirm the discrimination of several histologically defined subgroups of pineal tumors and further delineate distinct subtypes based on DNA methylation analysis. Focusing in more detail on PB, this study is one of the first reports presenting a classification of distinct PB subtypes and newly described molecular subgroups arising in the pineal gland.

With PB occurring on the basis of *RB1* germline alterations in the context of 'trilateral retinoblastoma' syndrome, a relation of PB and RB was previously known. Accordingly, we identified a distinct molecular subgroup Pin-RB with either somatic or germline *RB1* alterations that share remarkable similarities with the RB methylation profile. These tumors occur at a notably younger age than the core PB subtypes PB-Grp1A, PB-Grp1B and PB-Grp2 (similar to the mean age at diagnosis for RB [9]), and frequently show common features of RB like loss of chromosome 16 and gain of chromosome 1q [2, 17, 18, 28, 29].

Similarly, further clinical characterization is necessary for the newly described molecular subgroup PB-MYC. *MYC* gain as well as chromosome 8p and 10q loss as recurrently observed in PB-MYC tumors are known alterations in MB-G3 [34]. Even though the distinct PB subgroup PB-MYC shares some molecular features with MB, it can still be distinguished based on location as well as further clinical, histopathological and molecular features. PB-MYC show unique characteristics in contrast to the three core PB subtypes, including younger age at diagnosis, similarities to MB-G3 based on DNA methylation analysis and copy-number profiles, absence of alterations in the miRNA processing pathway, as well as poor outcome. Our data with the combination of a high proportion of infants and shorter overall survival in the PB-MYC subgroup can lead to the hypothesis that the underlying biology of this molecular subgroup might explain the observation of young age as a negative prognostic factor in PB [32, 36].

Alterations in the miRNA processing pathway are described in different pediatric tumor entities, like pleuropulmonary blastoma, but also Sertoli-Leydig cell tumor of the ovary, embryonal rhabdomyosarcoma, primary intracranial sarcoma and PB in the context of underlying *DICER1* germline mutations [8, 24, 40, 41]. Furthermore, mutations in *DROSHA*, *DGCR8* and *DICER1* are found in Wilms tumor [14, 46]. MiRNAs as a class of non-coding RNAs are considered to be involved in the development
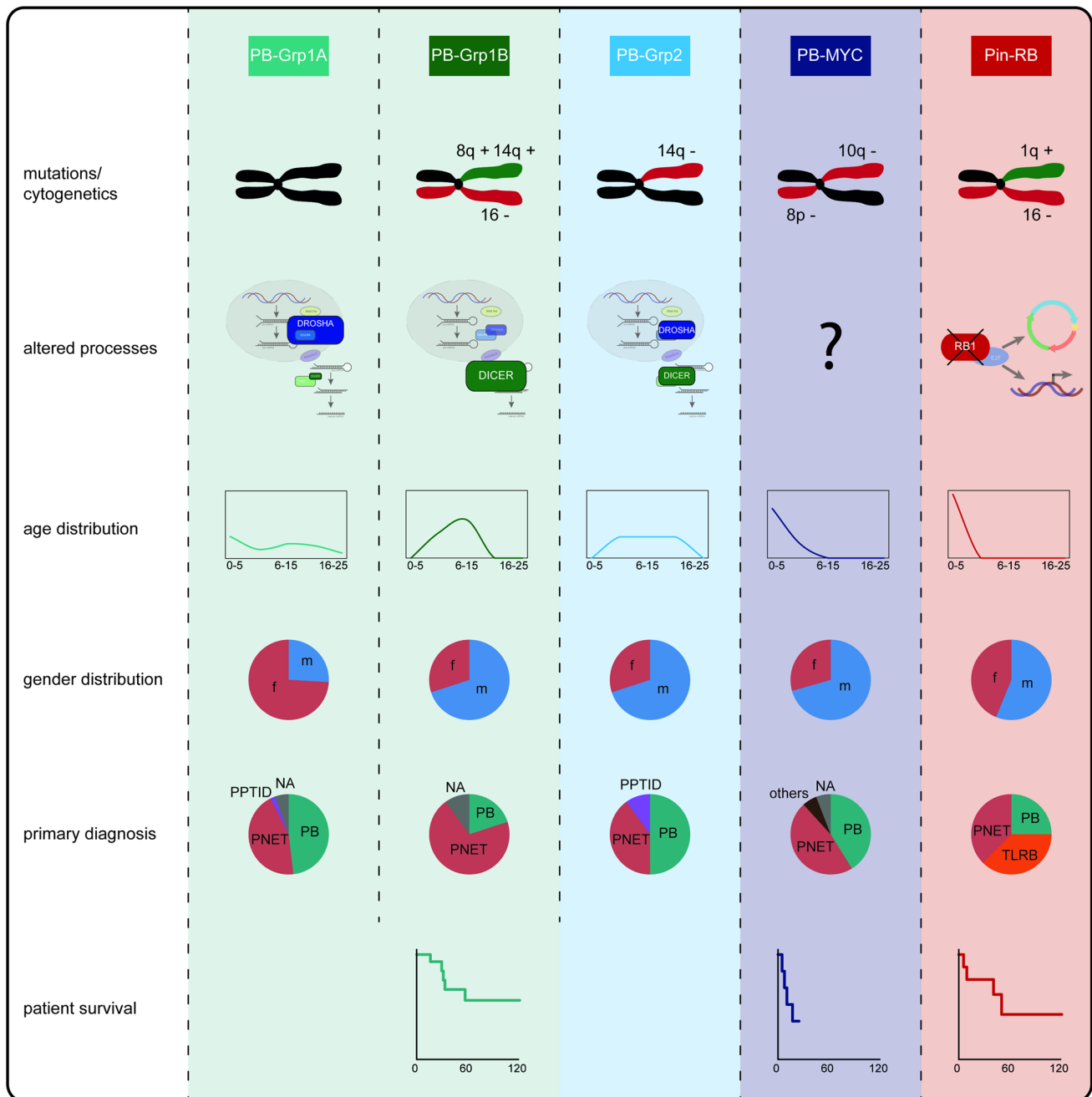
Fig. 5 Illustrative summary of distinct clinical and molecular characteristics of the pineoblastoma subtypes and well as Pin-RB and PB-MYC subgroups

of cancer, e.g., through dysregulation of tumor-suppressive miRNAs or activation of miRNAs with oncogenic function [37]. *DICER1* alterations affect the processing of pre-miRNA hairpins, for example with missense mutations located in the Ribonuclease IIIB domain leading to depletion of mature 5′ miRNA [1, 11]. Interestingly, the *DICER1* mutated cases in our cohort did not show a depletion of 5′ miRNA, most likely due to the detected mutations not affecting the Ribonuclease IIIB domain.

The specific impact of distinct alterations in the different genes of the miRNA processing pathway in PB needs to be investigated in a larger cohort facilitating miRNA- as well as total RNA sequencing.

In conclusion, with the current study we present a molecular subgrouping (summarized in Fig. 5) of tumors of the pineal region correlating with distinct clinical features and genetic alterations. In particular, three core subtypes of PB are described in which alterations in the miRNA processing

pathway are the predominant characteristic. Furthermore, we shed light on the similarity of Pin-RB with retinoblastoma, hinting at common developmental origins, and introduce a new MB-like molecular subgroup (PB-MYC) associated with a poor prognosis. These results may help to define a more rational patient stratification into clinical trials in future, as a basis for treatment optimization particularly with more targeted therapeutic approaches. Further functional characterization of miRNA processing alterations, histopathological reviews as well as clinical follow-up studies are now required to build upon the foundation presented here.

References

1. Anglesio MS, Wang Y, Yang W, Senz J, Wan A, Heravi-Moussavi A et al (2013) Cancer-associated somatic DICER1 hotspot mutations cause defective miRNA processing and reverse-strand expression bias to predominantly mature 3p strands through loss of 5p strand cleavage. J Pathol 229:400–409. https://doi.org/10.1002/path.4135

2. Blanquet V, Turleau C, Gross-Morand MS, Senamaud-Beaufort C, Doz F, Besmond C (1995) Spectrum of germline mutations in the RB1 gene: a study of 232 patients with hereditary and non hereditary retinoblastoma. Hum Mol Genet 4:383–388. https://doi.org/10.1093/hmg/4.3.383

3. Bohrnsen F, Enders C, Ludwig HC, Bruck W, Fuzesi L, Gutenberg A (2015) Common molecularcytogenetic alterations in tumors originating from the pineal region. Oncol Lett 10(3):1853–1857. https://doi.org/10.3892/ol.2015.3383

4. Capper D, Jones DTW, Sill M, Hovestadt V, Schrimpf D, Sturm D et al (2018) DNA methylation-based classification of central nervous system tumours. Nature 555:469–474. https://doi.org/10.1038/nature26000

5. Consortium EP (2012) An integrated encyclopedia of DNA elements in the human genome. Nature 489:57–74. https://doi.org/10.1038/nature11247

6. de Jong MC, Kors WA, de Graaf P, Castelijns JA, Kivela T, Moll AC (2014) Trilateral retinoblastoma: a systematic review and meta-analysis. Lancet Oncol 15:1157–1167. https://doi.org/10.1016/S1470-2045(14)70336-5

7. de Jong MC, Kors WA, de Graaf P, Castelijns JA, Moll AC, Kivela T (2015) The incidence of trilateral retinoblastoma: a systematic review and meta-analysis. Am J Ophthalmol 160(1116–1126):e5. https://doi.org/10.1016/j.ajo.2015.09.009

8. de Kock L, Sabbaghian N, Druker H, Weber E, Hamel N, Miller S et al (2014) Germ-line and somatic DICER1 mutations in pineoblastoma. Acta Neuropathol 128:583–595. https://doi.org/10.1007/s00401-014-1318-7

9. Dimaras H, Kimani K, Dimba EA, Gronsdahl P, White A, Chan HS et al (2012) Retinoblastoma. Lancet 379:1436–1446. https://doi.org/10.1016/S0140-6736(11)61137-9

10. Farnia B, Allen PK, Brown PD, Khatua S, Levine NB, Li J et al (2014) Clinical outcomes and patterns of failure in pineoblastoma: a 30-year, single-institution retrospective review. World neurosurg 82:1232–1241. https://doi.org/10.1016/j.wneu.2014.07.010

11. Foulkes WD, Priest JR, Duchaine TF (2014) DICER1: mutations, microRNAs and mechanisms. Nat Rev Cancer 14:662–672. https://doi.org/10.1038/nrc3802

12. Frankish A, Diekhans M, Ferreira AM, Johnson R, Jungreis I, Loveland J et al (2019) GENCODE reference annotation for the human and mouse genomes. Nucleic Acids Res 47:D766–D773. https://doi.org/10.1093/nar/gky955

13. Friedrich C, von Bueren AO, von Hoff K, Gerber NU, Ottensmeier H, Deinlein F et al (2013) Treatment of young children with CNS-primitive neuroectodermal tumors/pineoblastomas in the prospective multicenter trial HIT 2000 using different chemotherapy regimens and radiotherapy. Neuro Oncol 15:224–234. https://doi.org/10.1093/neuonc/nos292

14. Gadd S, Huff V, Walz AL, Ooms A, Armstrong AE, Gerhard DS et al (2017) A Children's Oncology Group and TARGET initiative exploring the genetic landscape of Wilms tumor. Nat Genet 49:1487–1494. https://doi.org/10.1038/ng.3940

15. Gerber NU, von Hoff K, Resch A, Ottensmeier H, Kwiecien R, Faldum A et al (2014) Treatment of children with central nervous system primitive neuroectodermal tumors/pinealoblastomas in the prospective multicentric trial HIT 2000 using hyperfractionated radiation therapy followed by maintenance chemotherapy. Int J Radiat Oncol Biol Phys 89:863–871. https://doi.org/10.1016/j.ijrobp.2014.04.017

16. Goschzik T, Gessi M, Denkhaus D, Pietsch T (2014) PTEN mutations and activation of the PI3K/Akt/mTOR signaling pathway in papillary tumors of the pineal region. J Neuropathol Exp Neurol 73:747–751. https://doi.org/10.1097/NEN.0000000000000093

17. Gratias S, Schuler A, Hitpass LK, Stephan H, Rieder H, Schneider S et al (2005) Genomic gains on chromosome 1q in retinoblastoma: consequences on gene expression and association with clinical manifestation. Int J Cancer 116:555–563. https://doi.org/10.1002/ijc.21051

18. Gustmann S, Klein-Hitpass L, Stephan H, Weber S, Bornfeld N, Kaulisch M et al (2011) Loss at chromosome arm 16q in retinoblastoma: confirmation of the association with diffuse vitreous seeding and refinement of the recurrently deleted region. Genes Chromosomes Cancer 50:327–337. https://doi.org/10.1002/gcc.20857

19. Heim S, Sill M, Jones DT, Vasiljevic A, Jouvet A, Fevre-Montange M et al (2016) Papillary tumor of the pineal region: a distinct molecular entity. Brain Pathol 26:199–205. https://doi.org/10.1111/bpa.12282

20. Heravi-Moussavi A, Anglesio MS, Cheng SW, Senz J, Yang W, Prentice L et al (2012) Recurrent somatic DICER1 mutations in nonepithelial ovarian cancers. N Engl J Med 366:234–242. https://doi.org/10.1056/NEJMoa1102903

21. Hwang EI, Kool M, Burger PC, Capper D, Chavez L, Brabetz S et al (2018) Extensive molecular and clinical heterogeneity in patients with histologically diagnosed CNS-PNET treated as a single entity: a report from the Children's Oncology Group Randomized ACNS0332 Trial. J Clin Oncol. https://doi.org/10.1200/JCO.2017.76.4720

22. Kaatsch P, Grabow D, Spix C (2018) German Childhood Cancer Registry—annual report 2018 (1980–2017). https://www.kinderkrebsregister.de/typo3temp/secure_downloads/22605/0/2df4719687ba2596d4216218a4f4632763b64847/jb2018s.pdf. Accessed 7 Nov 2019

23. Kline CN, Joseph NM, Grenert JP, van Ziffle J, Talevich E, Onodera C (2017) Targeted next-generation sequencing of pediatric neuro-oncology patients improves diagnosis, identifies pathogenic germline mutations, and directs targeted therapy. Neuro Oncol 19(5):699–709. https://doi.org/10.1093/neuonc/now254

24. Koelsche C, Mynarek M, Schrimpf D, Bertero L, Serrano J, Sahm F et al (2018) Primary intracranial spindle cell sarcoma with rhabdomyosarcoma-like features share a highly distinct methylation profile and DICER1 mutations. Acta Neuropathol 136:327–337. https://doi.org/10.1007/s00401-018-1871-6

25. Kozomara A, Griffiths-Jones S (2011) miRBase: integrating microRNA annotation and deep-sequencing data. Nucleic Acids Res 39:D152–157. https://doi.org/10.1093/nar/gkq1027

26. Lee JC, Mazor T, Lao R, Wan E, Diallo AB, Hill NS et al (2019) Recurrent KBTBD4 small in-frame insertions and absence of DROSHA deletion or DICER1 mutation differentiate pineal parenchymal tumor of intermediate differentiation (PPTID) from pineoblastoma. Acta Neuropathol. https://doi.org/10.1007/s00401-019-01990-5

27. Li MH, Bouffet E, Hawkins CE, Squire JA, Huang A (2005) Molecular genetics of supratentorial primitive neuroectodermal tumors and pineoblastoma. Neurosurg Focus 19:E3

28. Lillington DM, Kingston JE, Coen PG, Price E, Hungerford J, Domizio P et al (2003) Comparative genomic hybridization of 49 primary retinoblastoma tumors identifies chromosomal regions associated with histopathology, progression, and patient outcome. Genes Chromosomes Cancer 36:121–128. https://doi.org/10.1002/gcc.10149

29. Lohmann DR (1999) RB1 gene mutations in retinoblastoma. Hum Mutat 14:283–288. https://doi.org/10.1002/(SICI)1098-1004(199910)14:4%3c283:AID-HUMU2%3e3.0.CO;2-J

30. Louis DN, Ohgaki H, Wiestler OD, Cavenee WK (eds) (2016) WHO classification of tumour of the central nervous system, 4th edn. IARC, Lyon

31. Miller S, Rogers HA, Lyon P, Rand V, Adamowicz-Brice M, Clifford SC et al (2011) Genome-wide molecular characterization of central nervous system primitive neuroectodermal tumor and pineoblastoma. Neuro Oncol 13:866–879. https://doi.org/10.1093/neuonc/nor070

32. Mynarek M, Pizer B, Dufour C, van Vuurden D, Garami M, Massimino M et al (2017) Evaluation of age-dependent treatment strategies for children and young adults with pineoblastoma: analysis of pooled European Society for Paediatric Oncology (SIOP-E) and US Head Start data. Neuro Oncol 19:576–585. https://doi.org/10.1093/neuonc/now234

33. Northcott PA, Buchhalter I, Morrissy AS, Hovestadt V, Weischenfeldt J, Ehrenberger T et al (2017) The whole-genome landscape of medulloblastoma subtypes. Nature 547:311–317. https://doi.org/10.1038/nature22973

34. Northcott PA, Shih DJ, Peacock J, Garzia L, Morrissy AS, Zichner T et al (2012) Subgroup-specific structural variation across 1,000 medulloblastoma genomes. Nature 488:49–56. https://doi.org/10.1038/nature11327

35. Ostrom QT, Gittleman H, Truitt G, Boscia A, Kruchko C, Barnholtz-Sloan JS (2018) CBTRUS statistical report: primary brain and other central nervous system tumors diagnosed in the United States in 2011–2015. Neuro Oncol 20:iv1–iv86. https://doi.org/10.1093/neuonc/noy131

36. Parikh KA, Venable GT, Orr BA, Choudhri AF, Boop FA, Gajjar AJ et al (2017) Pineoblastoma—the experience at St Jude Children's Research Hospital. Neurosurgery 81:120–128. https://doi.org/10.1093/neuros/nyx005

37. Rupaimoole R, Slack FJ (2017) MicroRNA therapeutics: towards a new era for the management of cancer and other diseases. Nat Rev Drug Discov 16:203–222. https://doi.org/10.1038/nrd.2016.246

38. Sahm F, Schrimpf D, Jones DT, Meyer J, Kratz A, Reuss D et al (2016) Next-generation sequencing in routine brain tumor diagnostics enables an integrated diagnosis and identifies actionable targets. Acta Neuropathol 131:903–910. https://doi.org/10.1007/s00401-015-1519-8

39. Schild SE, Scheithauer BW, Schomberg PJ, Hook CC, Kelly PJ, Frick L et al (1993) Pineal parenchymal tumors. Clinical, pathologic, and therapeutic aspects. Cancer 72:870–880

40. Schultz KA, Yang J, Doros L, Williams GM, Harris A, Stewart DR et al (2014) DICER1-pleuropulmonary blastoma familial tumor predisposition syndrome: a unique constellation of neoplastic conditions. Pathol Case Rev 19:90–100. https://doi.org/10.1097/PCR.0000000000000027

41. Schultz KAP, Rednam SP, Kamihara J, Doros L, Achatz MI, Wasserman JD et al (2017) PTEN, DICER1, FH, and their associated tumor susceptibility syndromes: clinical features, genetics, and surveillance recommendations in childhood. Clin Cancer Res 23(12):e76–e82. https://doi.org/10.1158/1078-0432.CCR-17-0629

42. Shukla GC, Singh J, Barik S (2011) MicroRNAs: processing, maturation, target recognition and regulatory functions. Mol Cell Pharmacol 3:83–92

43. Snuderl M, Kannan K, Pfaff E, Wang S, Stafford JM, Serrano J et al (2018) Recurrent homozygous deletion of DROSHA and microduplication of PDE4DIP in pineoblastoma. Nat Commun 9:2868. https://doi.org/10.1038/s41467-018-05029-3

44. Sturm D, Orr BA, Toprak UH, Hovestadt V, Jones DTW, Capper D et al (2016) New brain tumor entities emerge from molecular classification of CNS-PNETs. Cell 164:1060–1072. https://doi.org/10.1016/j.cell.2016.01.015

45. von Bueren AO, Gerss J, Hagel C, Cai H, Remke M, Hasselblatt M (2012) DNA copy number alterations in central primitive neuroectodermal tumors and tumors of the pineal region: an international individual patient data meta-analysis. J Neurooncol 109(2):415–423. https://doi.org/10.1007/s11060-012-0911-7

46. Wegert J, Ishaque N, Vardapour R, Georg C, Gu Z, Bieg M et al (2015) Mutations in the SIX1/2 pathway and the DROSHA/DGCR8 miRNA microprocessor complex underlie high-risk blastemal type Wilms tumors. Cancer Cell 27:298–311. https://doi.org/10.1016/j.ccell.2015.01.002

47. Worst BC, van Tilburg CM, Balasubramanian GP, Fiesel P, Witt R, Freitag A et al (2016) Next-generation personalised medicine for high-risk paediatric cancer patients—the INFORM pilot study. Eur J Cancer 65:91–101. https://doi.org/10.1016/j.ejca.2016.06.009

48. Yamanaka R, Hayano A, Takashima Y (2017) Trilateral retinoblastoma: a systematic review of 211 cases. Neurosurg Rev 42:39–48. https://doi.org/10.1007/s10143-017-0890-4

Affiliations

Elke Pfaff[1,2,3] · Christian Aichmüller[4] · Martin Sill[1,5] · Damian Stichel[6,7] · Matija Snuderl[8,9,10] ·
Matthias A. Karajannis[11] · Martin U. Schuhmann[12] · Jens Schittenhelm[13] · Martin Hasselblatt[14] · Christian Thomas[14] ·
Andrey Korshunov[6,7] · Marina Rhizova[15] · Andrea Wittmann[1,2] · Anna Kaufhold[1,5] · Murat Iskar[4] · Petra Ketteler[16] ·
Dietmar Lohmann[17] · Brent A. Orr[18] · David W. Ellison[18,19] · Katja von Hoff[20,21] · Martin Mynarek[21] ·
Stefan Rutkowski[21] · Felix Sahm[1,6,7] · Andreas von Deimling[6,7] · Peter Lichter[4,22] · Marcel Kool[1,5] · Marc Zapatka[4] ·
Stefan M. Pfister[1,3,5] · David T. W. Jones[1,2]

[1]   Hopp Children's Cancer Center Heidelberg (KiTZ), Heidelberg, Germany

[2]   Pediatric Glioma Research Group (B360), German Cancer Research Center (DKFZ), Hopp Children's Cancer Center Heidelberg (KiTZ), Heidelberg, Germany

[3]   Department of Pediatric Oncology, Hematology and Immunology, Heidelberg University Hospital, Heidelberg, Germany

[4]   Division of Molecular Genetics, German Cancer Research Center (DKFZ), Heidelberg, Germany

[5]   Division of Pediatric Neurooncology, German Cancer Research Center (DKFZ), Heidelberg, Germany

[6]   Department of Neuropathology, Institute of Pathology, University Hospital Heidelberg, Heidelberg, Germany

[7]   Clinical Cooperation Unit Neuropathology, German Cancer Research Center (DKFZ), German Consortium for Translational Cancer Research (DKTK), Heidelberg, Germany

[8]   Division of Neuropathology, NYU Langone Health, New York, USA

[9]   Laura and Isaac Perlmutter Cancer Center, NYU Langone Health, New York, USA

[10]   Division of Molecular Pathology and Diagnostics, NYU Langone Health, New York, USA

[11]   Department of Pediatrics, Memorial Sloan Kettering Cancer Center, New York, USA

[12]   Division of Pediatric Neurosurgery, Department of Neurosurgery, Eberhard Karl's University Hospital of Tübingen, Tübingen, Germany

[13]   Institute of Neuropathology, Department of Pathology and Neuropathology, University of Tübingen, Comprehensive Cancer Center Tübingen-Stuttgart, Tübingen, Germany

[14]   Institute of Neuropathology, University Hospital Münster, Munster, Germany

[15]   Department of Neuropathology, Burdenko Neurosurgical Institute, Moscow, Russia

[16]   Pediatrics III, Pediatric Oncology and Hematology, University Hospital Essen, Essen, Germany

[17]   Eye Cancer Genetics, Institute of Human Genetics, University Hospital Essen, Essen, Germany

[18]   Department of Pathology, St. Jude Children's Research Hospital, Memphis, USA

[19]   Department of Oncology, St. Jude Children's Research Hospital, Memphis, USA

[20]   Department of Pediatric Oncology/Hematology, Charité-Universitätsmedizin Berlin, Berlin, Germany

[21]   Department of Paediatric Haematology and Oncology, University Medical Centre Hamburg-Eppendorf, Hamburg, Germany

[22]   German Cancer Consortium (DKTK), German Cancer Research Center (DKFZ), Heidelberg, Germany